Available online at www.sciencedirect.com
SCIENCE DIRECT®
Advances in Water Resources 26 (2003) 925–937
Advances in Water Resources
www.elsevier.com/locate/advwatres

Comparing transient storage modeling and residence time distribution (RTD) analysis in geomorphically varied reaches in the Lookout Creek basin, Oregon, USA

Michael N. Gooseff [a,*], Steve M. Wondzell [b], Roy Haggerty [a], Justin Anderson [c]

[a] Department of Geosciences, 104 Wilkinson Hall, Oregon State University, Corvallis, OR 97331-5506, USA
[b] US Forest Service, Pacific Northwest Research Station, Olympia Forestry Sciences Lab, 3625 93rd Ave. SW, Olympia, WA 98512, USA
[c] Department of Forest Sciences, Oregon State University, 321 Richardson Hall, Corvallis, OR 97331-5752, USA

Received 15 February 2002; accepted 15 May 2003

Abstract

The stream tracer technique has been widely used as a method of characterizing hyporheic exchange in stream-catchment studies, commonly incorporating the use of the numerical, transient storage model OTIS, which assumes an exponential residence time distribution. In this study, we compare OTIS and, a model that admits a general residence time distribution (RTD), called solute transport and multirate mass transfer-linear coordinates (STAMMT-L). Models were compared using slug-tracer injections of rhodamine WT (RWT) in three geomorphically distinct stream reaches in the Lookout Creek basin, Oregon USA: a second-order reach of a stream in Watershed 3 which is characterized by pool-step morphology; and two fourth-order reaches of Lookout Creek, one characterized by a single-thread, pool-step morphology, the other a morphologically complex reach with braided channels. OTIS modeling results tended to match short time scale concentrations well, including the advective peak, but the simulated late-time RTD of stream RWT concentrations was in error. The STAMMT-L model allowed for more accurate characterization of late-time stream RWT concentrations, and so characterized a larger portion of the entire RTD. Although both models are sensitive to morphologic differences among the studied stream reaches, they are also clearly different in the relative importance placed on short vs. long residence time distributions. Consequently the two models will result in different views of the hyporheic zone and its role in stream ecosystem processes.

Keywords: Solute transport; Hyporheic zone; Numerical simulation; Residence time distribution

1. Introduction

The hyporheic zone has been defined as a subsurface flow path adjacent to a stream, roughly parallel to the downstream direction of a stream, along which recent stream water will mix with subsurface water and soon return to the stream [20]. As Bencala [3] points out, hyporheic exchange increases stream water residence times in watersheds. A variety of hyporheic flow paths may exist in any stream reach, thus creating a distribution of residence times for stream solutes. The shortest residence times are defined by mean stream flow velocity, the longest by long time scale exchange between the stream and the hyporheic zone. The characterization of hyporheic exchange and its effect on transport and fate of solutes of biogeochemical interest has been the subject of numerous studies [2,6–8,12,35,38,47]. Hyporheic exchange is driven by hydraulic head gradients between streams and adjoining saturated streambed material, and several studies have approached hyporheic exchange modeling from a groundwater flow or hydraulic head distribution perspective [9,10,23,25,32,36,40,46,49]. A more popular approach used by hydrologists and stream ecologists is to use some modified form of the stream solute advection dispersion model, such as the transient storage model put forth by Bencala and Walters [4], and similar models by Jackman et al. [24], and Hart [19]. These models account for stream transport mechanisms (dispersion and advection), lateral inflow and outflow, and transient storage, a transport

* Corresponding author. Present address: Department of Aquatic, Watershed, and Earth Resources, Utah State University, Logan, UT 84322-5210, USA. Tel.: +435-797-8292; fax: +435-797-1871.
E-mail address: michael.gooseff@usu.edu (M.N. Gooseff).

0309-1708/$ - see front matter © 2003 Elsevier Ltd. All rights reserved.
doi:10.1016/S0309-1708(03)00105-2

mechanism that should have a unique mean time scale in a well-designed stream tracer experiment [21].

Current forms of the modified advection–dispersion equations implicitly assume that the residence time distribution (RTD) of water (solute) in storage is exponential. Harvey et al. [21] found this to be a limiting factor in trying to accurately determine hyporheic solute arrival times at particular sub-stream locations. Further, Harvey et al. [21] point out that the time scale of exchange identified by the stream tracer technique and subsequent modeling with modified advection–dispersion equations results in mean hyporheic residence times that are on the order of the temporal length of the tracer experiment. This is a significant limitation of the transient storage model, as it only characterizes hyporheic flow paths over a relatively narrow range of short timescales, and the range of timescales is as much an artifact of experimental design as it is a result of physical attributes of the studied stream reach [18].

Recently, a few studies have characterized hyporheic exchange using general RTD modeling instead of the transient storage model [18,48]. General RTD modeling fits a simulated breakthrough curve to stream tracer data, but is not bound by an exponential RTD assumption. Instead, any RTD can be fit to the observed data. For example, Wörman et al. [48] found that a log-normal RTD best fit transport data from Säva Brook, Sweden, and Haggerty et al. [18] found that a power-law RTD best described rhodamine WT (RWT) data in a second-order stream in Oregon, USA. Although these techniques have been applied before in groundwater modeling [15,16], applications of RTD fitting to stream-solute transport is relatively new.

In this paper, we compare results of three RWT slug tracer experiments in three geomorphically distinct stream reaches in the Lookout Creek basin in central Oregon, USA. We simulate RWT transport using a modified advection–dispersion equation approach with an exponential RTD, and by applying a model that fits a general RTD to the observations. We suggest that the a priori assumption of an exponential RTD applied to many tracer experiments may not be appropriate. Further, we suggest that the consequence of inappropriate RTD classification, or applying an RTD that does not closely track the observed data, leads to incorrect conclusions about long-term transport and fate of stream solutes.

2. Study sites

2.1. Study site description

The Lookout Creek watershed, located in central Oregon, USA, comprises the H.J. Andrews Experimental Forest. The streams of the 64 km^2 watershed have been subjects of several papers investigating stream ecosystem dynamics [14,41,44], and hyporheic zone dynamics [7,18,25,46,47]. This study focused on three stream reaches. The first, WS03, is a second-order, single-thread channel draining Watershed 3, a 100 ha headwater stream basin. The channel has been repeatedly scoured by debris flows originating from landslides within the watershed, the most recent of which occurred in 1996. The study reach is 306.4 m in length, and contains large boulders, logs and other colluvium deposited during the 1996 debris flows (Fig. 1A). The average gradient within the reach is 12.6%, and sinuosity averages 1.13. Additional site description can be found in [18,25].

The upper fourth-order reach, LO410, is a single thread alluvial channel with a step-pool/step-riffle morphology (Fig. 1B). Basin area at the head of the reach is approximately 25.9 km^2. The length of the studied reach is 212.2 m and has an average gradient of 4.84% and average sinuosity of 1.17. The lower fourth-order reach, LO411, is a braided alluvial channel immediately downstream of LO410 that terminates at a channel-spanning bedrock outcrop (Fig. 1C). Basin area at the head of the reach is approximately 26.0 km^2. The length of the studied reach is 379.2 m and has an average gradient of 4.00% and average sinuosity of 1.19. The combined reach length of LO410 and LO411 is 591.4 m and has an average gradient of 4.26%.

2.2. Lookout Creek basin geomorphology

Montgomery and Buffington [29] conceptualize a continuum of alluvial channel-reach morphologies ranging in the down-valley direction from cascade to step-pool to plane bed to pool-riffle. Stream reaches in this study area generally fall along this continuum, though often stream reaches cannot be classified exclusively into one of the above categories. Riffle-step morphologies occur where the step-pool morphology is poorly developed. Split channels, and braided channels occur in the proximity of log jams. Where step-pool and pool-riffle morphologies exist, they are influenced by the presence of wood, boulders or bedrock outcrops.

Valley morphology in the Lookout Creek basin varies from sections with a broad floodplain to sections constrained by alluvial fans, debris flows, and hillslope processes, to sections with narrow bedrock gorges. Narrowest valley floor widths occur at bedrock gorges and where alluvial fans force the stream channel against the opposite bedrock valley wall, and the highest valley floor width index values occur upstream of these constrained reaches where valley floors aggrade and little bedrock is exposed [13]. This aggradation locally reduces the stream gradient, and widens and thickens the alluvium beneath the stream.

Detailed maps and longitudinal profiles of portions of the Lookout Creek basin reveal that alternating

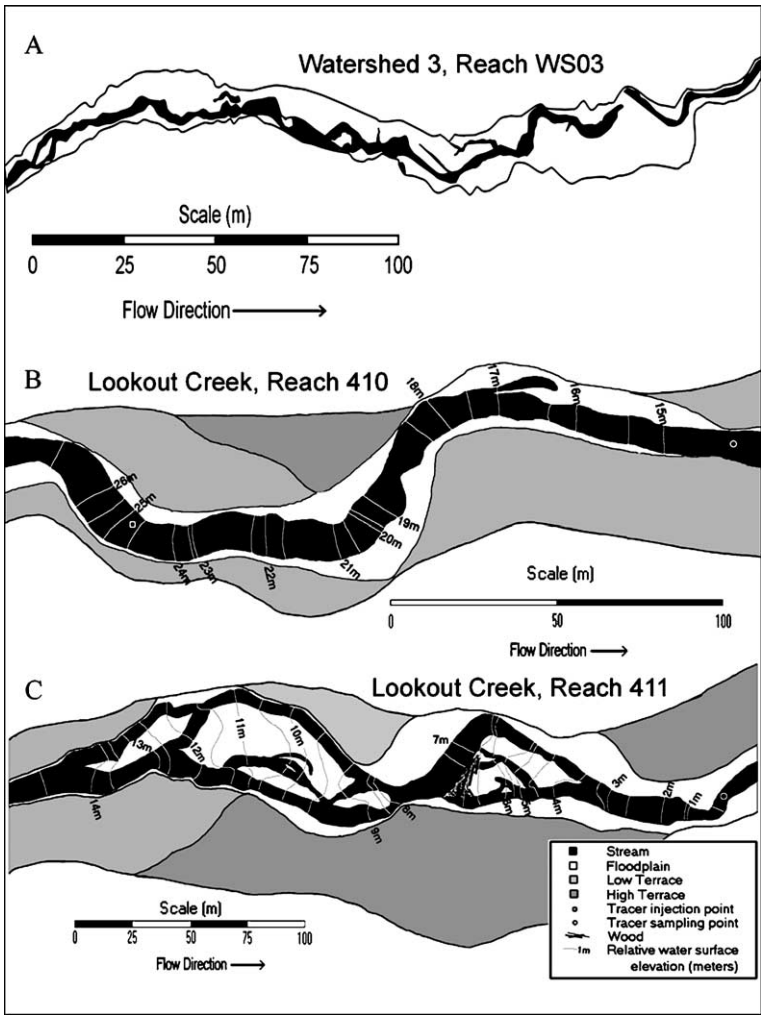

Fig. 1. Location maps for experimental stream reaches in: (A) WS03; (B) LO410 and (C) LO411. Water surface elevations (0.5 m interval) were surveyed in-stream, and estimated for subsurface regions between channels in (B) and (C).

constrained and unconstrained stream segments are characterized by corresponding segments of high and low gradient, respectively, and that the dimensions of pool-riffle features, and other fluvially formed features, increase with increasing catchment area. Where bedrock is not present in the channel bottom, the alternating segments of high and low gradient are likely the result of sediment aggradation.

3. Methods

3.1. Stream survey methods

Stream reaches were surveyed with a Topcon [1] AT-G3 auto level and rod (Topcon, Inc., Pleasanton, CA). A fiberglass measuring tape was stretched between steel stakes driven into the streambed along the thalweg. Streambed elevations and water-surface elevations, relative to an arbitrary benchmark, were surveyed at points along the measuring tape. The spacing interval between survey points varied to capture channel-spanning breaks in the slope of the bed and water surface. Stream-channel widths, floodplain widths, and terrace widths were measured at 10 m intervals. The boundary between the floodplain and active channel was identified by the break between bare alluvium and surfaces occupied by well-established perennial vegetation. Maps of the stream reaches were drawn using a combination of survey data, and width measurements. Tracer injection and monitoring points were surveyed at a later date, and added to the existing maps. Sinuosity was calculated from the map as the thalweg length divided by the straight-line distance along the valley axis for each reach. Source area for each reach was calculated from a 10-m digital elevation model (DEM).

[1] The use of trade or firm names in the publication is for reader information and does not imply endorsement by the US Department of Agriculture of any product or service.

3.2. Stream tracer experiments

Three slug tracer experiments were preformed. Eleven grams of RWT (Fomulabs[1], Piqua, OH) was injected into the WS03 stream reach on April 21, 2001. Stream flow, measured at a stream gauge at the bottom of the reach, was steady at 0.027 $m^3 s^{-1}$ for the first 15.7 h of the experiment, and then gradually declined to 0.026 $m^3 s^{-1}$ at 27 h (see [18]). On July 10, 2001, 10.4 g of RWT was injected at the head of the LO411 stream reach. Stream flow was measured to be 0.310 $m^3 s^{-1}$, at the end of the reach prior to the injection. Seventy-five grams of RWT (Bright Dyes[1], Miamisburg, OH) was injected at the head of the LO410–411 stream reaches on July 18, 2001. Stream flow was measured to be 0.259 and 0.263 $m^3 s^{-1}$, at the end of the LO411 reach at 14 h prior to the tracer experiment, and 10 h after the start of the experiment, respectively.

Early in each stream tracer experiment, RWT fluorescence data was collected at a downstream sample point using a Turner Designs[1] model 10AU field fluorometer (Turner Designs, Inc., Sunnyvale, CA) for WS03 and LO411, and a Turner Designs[1] Model 10-005 R field fluorometer for LO410. Both were set up with a flow-through cell. Data was collected on a 5 s interval for the first 28 h in WS03 and on a 10 s interval for the first 6.3 h (July 10 experiment) and 7 h (July 18 experiment) in LO411. At LO410, fluorometer readings were manually read every 60 s for the first 7 h of the experiment. For the remainder of the experiment, stream water samples were collected with programmable field autosamplers (ISCO[1], Inc., Lincoln, NE) for an additional 7 days in WS03 and 4 days in LO410 and LO411. Samples collected with autosamplers were analyzed with the same Turner Designs fluorometers in a lab within 24 h of retrieval.

3.3. Transient storage modeling

We used the computer model one-dimensional transport with inflow and storage (OTIS, http://co.water.usgs.gov/otis/) [34] to assess transient storage in the studied stream reaches. The RTD underlying the OTIS model is exponential. OTIS will be referred to as the exponential RTD throughout the methods and results sections of this paper. Exponential RTD modeling is governed by the following equations for the transport of RWT, assuming no net groundwater gains or losses:

$$\text{(in-stream)} \quad \frac{\partial C}{\partial t} = -\frac{Q}{A}\frac{\partial C}{\partial x} + D\frac{\partial^2 C}{\partial x^2} - \frac{A_S}{A}\frac{dC_S}{dt} - \lambda C \tag{1}$$

$$\text{(in-storage zone)} \quad \frac{dC_S}{dt} = \alpha\frac{A}{A_S}(C - C_S) - \lambda C_S \tag{2}$$

where A is the cross-sectional area of stream (m^2), A_S is the cross sectional area of storage zone (m^2), α is the first-order storage zone exchange coefficient (s^{-1}), C is the main channel solute concentration ($\mu g l^{-1}$), C_S is the storage zone solute concentration ($\mu g l^{-1}$), D is the dispersion coefficient ($m^2 s^{-1}$), x is the distance downstream (m), t is the time (s), Q is the stream flow rate ($m^3 s^{-1}$), and λ is the first-order uptake coefficient (s^{-1}). Recognizing that RWT is not a truly conservative tracer in stream systems [1], the first-order uptake coefficient λ was applied both in the stream and in the hyporheic zone to represent a uniform loss of RWT mass, similar to the approach reported by Runkel [34] modeling RWT data from Laenen and Risley [26].

3.4. General RTD modeling

General RTD modeling was conducted with the STAMMT-L model [17]. STAMMT-L applies a user-specified RTD to a general one-dimensional advection–dispersion transport equation

$$\frac{\partial C}{\partial t} = -v\frac{\partial C}{\partial x} + D\frac{\partial^2 C}{\partial x^2} - \beta_{tot}\frac{\partial C_S}{\partial t} \tag{3}$$

where v is the mean advection velocity, equivalent to Q/A ($m s^{-1}$), and β_{tot} is the ratio of storage to stream cross-sectional areas, equivalent to A_S/A. STAMMT-L represents dispersion as the mathematically equivalent product of the dispersivity and velocity, but in this paper we will compare dispersion in both models. In the general RTD model, the storage zone concentrations are defined as

$$\frac{\partial C_S}{\partial t} = \int_0^t \frac{\partial C(t-\tau)}{\partial t} g^*(\tau)\, d\tau \tag{4}$$

where τ is a lag time (s), and $g^*(t)$ may be defined with a distribution of exponential residence times

$$g^*(t) = \int_0^t \omega p(\omega) e^{-\omega t} d\omega \tag{5}$$

where ω is the a first-order mass-transfer rate coefficient, equivalent to $\alpha A/A_S$ (s^{-1}). The function $g^*(t)$ is the probability density that a tracer molecule entering the hyporheic zone at $t = 0$ will still be in the hyporheic zone at time t. In Eq. (5), $g^*(t)$ is generalized as a function of a distribution of exchange rates, $p(\omega)$. The density function $p(\omega)$ can take on different forms, corresponding to a particular RTD. For instance, a single first-order mass transfer RTD representation, equivalent to the exponential RTD above, is

$$g^*(t) = \omega e^{-\omega t} \tag{6}$$

For a power-law RTD, $g^*(t)$ takes on the form

$$g^*(t) = \frac{(k-2)}{(\omega_{max}^{k-2} - \omega_{min}^{k-2})} \int_{\omega_{min}}^{\omega_{max}} \omega^{k-2} e^{-\omega t} d\omega \tag{7}$$

where k is the power-law coefficient, which is given by the slope of late-time concentration tail. As pointed out by Haggerty et al. [16,18], a power-law concentration breakthrough curve scales as

$$C \sim t^{-k} \tag{8}$$

The general mean hyporheic residence time can be determined by the inverse of the harmonic mean of the exchange rates

$$t_S = \int_0^\infty \frac{p(\omega)}{\omega} d\omega \tag{9}$$

The governing equations of the general RTD model do not include a direct mass loss term for non-conservative solutes. Instead, a mass dilution factor is used

$$m_{rec} = \frac{m_{inj}}{\varphi} \tag{10}$$

where m_{rec} is the mass recovered, as simulated, at the end of the reach (g), m_{inj} is the mass injected (g), and φ is the total loss factor (–) due to irriversible sorption or by-passing.

For a particular RTD type, STAMMT-L solves the governing equations in the Laplace domain. Additional details are reported by Haggerty et al. [16]. Note, here we have replaced the α used by Haggerty et al. [16] with a ω, to reduce confusion between the transient storage model and general RTD parameter sets.

We have also calculated the scaled hyporheic residence probability density $g(t)$

$$g(t) = \beta_{tot} g^*(t) \tag{11}$$

Weighting $g^*(t)$ by β_{tot} allows comparison between models of the solute in the hyporheic zone at a given time. The value of $g(t)$ is best thought of as proportional to the amount of water taking at least time t to exchange with the stream. Haggerty et al. [16] refer to $g(t)$ as a memory function, because it accounts for the "memory" that the hyporheic zone has for tracer concentrations in the stream. To illustrate, a pulse of solute in the stream will be held in by the hyporheic zone in proportion to $g(t)$ over time t, thereby preserving the concentration information from the stream that is later released back to the stream.

3.5. Model parameter estimation

Parameter estimation of the exponential model for reaches WS03, and LO411 was accomplished using UCODE, a universal parameter estimation program [33], similar to the application described by Scott et al. [37]. For LO410, a best-fit parameter estimation was achieved and then modified to reduce the root mean squared error of the model fit, *and* visually match late-time breakthrough data. In the exponential model, A and D were parameterized initially, then fixed, and A_S, α, and λ were estimated in a second optimization run. Parameter estimation of the general RTD model was accomplished in log space using $\ln(C)$ values by using a non-linear least squares algorithm [27], which minimized the sum of squared residuals between simulated and observed values and is part of the STAMMT-L computer code. In the general RTD model, β_{tot}, D, k, v, and φ were estimated. In no case were observations (or simulated values) differentially weighted.

To provide a measure of "goodness of fit", the root mean squared error (RMSE) (similar to [22, p. 358]) was computed for each of the model simulations as

$$\mathrm{RMSE} = \sqrt{\frac{\sum_{i=1}^{n} \frac{(C_{sim} - C_{obs})^2}{C_{obs}^2}}{n}} \tag{12}$$

for n simulated observations. RMSE values close to 0 indicate a greater agreement between the simulated and observed data sets. Additionally, parameter estimate 95% confidence intervals, as computed by UCODE and STAMMT-L, are reported.

4. Results

4.1. WS03 results

The exponential RTD fits the observed tracer concentrations very well, from the start of the tracer injection through the passage of the advective peak (Fig. 2A), but fits the data poorly at late-time ($t > 1.0 \times 10^4$ s). The RMSE for the exponential RTD fit is 1.59. Optimal parameter values for the exponential RTD are presented in Table 1. Storage zone cross-sectional area, A_S, was found to be 5.3 times smaller than A, the cross-sectional area of the stream. Additionally, the mean hyporheic residence time, defined as $t_S = A_S/A\alpha$ [s] [39], calculated for the best-fit exponential model was 882 s.

As reported by Haggerty et al. [18], the model using a power-law RTD resulted in a much better fit to the observed RWT concentrations (Fig. 2B), having an RMSE of 0.09. The simulation presented here included a dilution, or mass loss function, of 1.13. Inclusion of dilution (mass loss) provided an improved fit to the observed data over the simulation reported by Haggerty et al. [18].

4.2. Lookout Creek results

Similar to the results from WS03, the exponential RTD adequately fit the data during the advective pulse (Figs. 3–5), but poorly fit the data at late-time in all cases, except in LO411 on July 18 (Fig. 5A). The exponential model RMSE values were found to be 0.97 for LO411 on July 10, 6.26 for LO410, and 0.99 for LO411 on July 18. The general RTD model showed that a

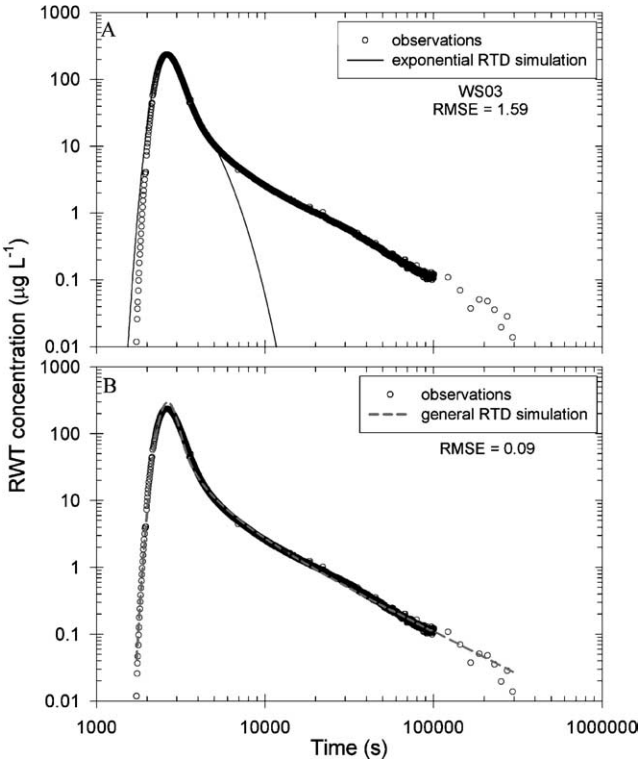

Fig. 2. WS03 stream tracer observations and simulation results for: (A) exponential RTD modeling and (B) general RTD modeling.

power-law RTD provided the better fit to the data for both reaches, all three simulations (Table 2), with RMSE values of 0.13 for LO411 on July 10, 0.43 for LO410, and 0.34 for LO411 on 18 July.

In the July 10 experiment in LO411, the exponential model was optimized with an α value of 9.82×10^{-3} s^{-1}, A_S of 1.137 m^2, and A_S/A ratio of 1.15 (Table 1). The general RTD model was optimized with a better fit using a β_{tot} value of 4.39, D value of 0.363 $m^2\,s^{-1}$, a dilution factor of 1.23, and the largest k value reported here, 1.58 (Table 2).

In LO410, the ratio of transient storage to stream cross-sectional area (A_S/A) was found to be 0.35, and α was found to be 1.74×10^{-4} s^{-1} (Table 1). The general RTD model was optimized with β_{tot} of 2.54, and a D of 0.573 $m^2\,s^{-1}$—the lowest observed among the three stream reaches studied. The reach also had a k value of 1.55, and the largest dilution factor of the simulations presented here, 1.29.

In the July 18 experiment in LO411, the exponential model was optimized with α of 1.84×10^{-4} s^{-1}, A_S of 4.51 m^2, and an A_S/A ratio of 2.95, the largest of the four simulations presented. The general RTD model was optimized with no mass losses (dilution set to 1.0), a β_{tot} value of 86.09 the largest of the four simulations presented, and a D of 0.275 $m^2\,s^{-1}$.

In the July 18 experiment in LO411, the exponential RTD model suggests that both the relative size of the hyporheic zone, (A_S/A) and the residence time of stream water in the hyporheic zone t_S were the largest of the reaches studied. Similarly, the general RTD model, using a power-law RTD, resulted in a somewhat better fit and the largest β_{tot} value of the four simulations presented. A dilution factor of 1.0 (no dilution) was used for the general RTD model, and a λ value of 0.0 was used in the exponential RTD model because there was

Table 1
Parameter estimates and computed metrics for exponential RTD model for WS03 and Lookout Creek

Parameter	Parameter/metric value			
	WS03	LO411 (July 10, 2001)	LO410 (July 18, 2001)	LO411 (July 18, 2001)
Q ($m^3\,s^{-1}$)	0.027	0.310	0.261	0.261
D ($m^2\,s^{-1}$)	0.273	0.055	0.575	0.863
	$[-0.56\pm0.04]$	$[-1.26\pm0.55]$	$[-2.40\pm0.44]$	$[-0.06\pm0.07]$
α (s^{-1})	2.15×10^{-4}	9.82×10^{-3}	1.74×10^{-4}	1.84×10^{-4}
	$[-3.67\pm0.05]$	$[-2.01\pm0.12]$	$[-3.76\pm2.76]$	$[-3.74\pm0.06]$
A (m^2)	0.234	0.985	1.22	1.53
	$[-0.63\pm0.01]$	$[-0.07\pm0.08]$	$[0.09\pm0.19]$	$[0.19\pm0.02]$
A_S (m^2)	0.044	1.137	0.423	4.51
	$[-1.35\pm0.06]$	$[-0.06\pm0.08]$	$[-0.37\pm4.21]$	$[0.65\pm0.13]$
λ (s^{-1})	1.45×10^{-4}	3.17×10^{-3}	5.86×10^{-4}	0.0[a]
	$[-3.84\pm0.04]$	$[-2.50\pm0.03]$	$[-3.23\pm1.52]$	
Metric				
v ($m\,s^{-1}$)[b]	0.155	0.316	0.213	0.170
A_S/A	0.188	1.15	0.347	2.95
t_S (s)	882	118	1991	3585
Model fit				
RMSE	1.59	0.97	6.26	0.99

Values in brackets represent log(parameter value) ±95% confidence interval.
[a] Sorption loss for LO411 on July 18 was set to 0.0.
[b] v is computed as Q/A.

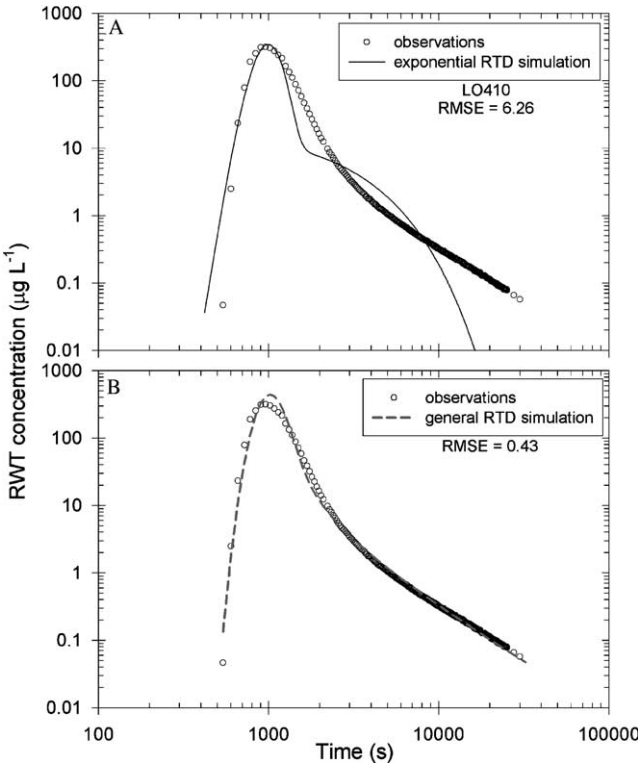

Fig. 3. LO410 stream tracer observations and simulation results from July 18, 2001 RWT stream tracer experiment for: (A) exponential RTD modeling and (B) general RTD modeling.

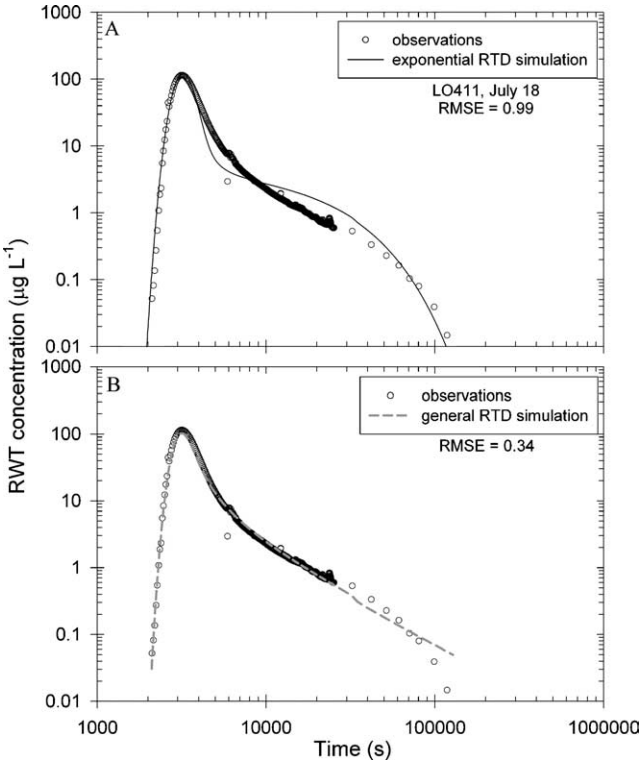

Fig. 5. LO411 stream tracer observations and simulation results from July 18, 2001 RWT stream tracer experiment for: (A) exponential RTD modeling and (B) general RTD modeling.

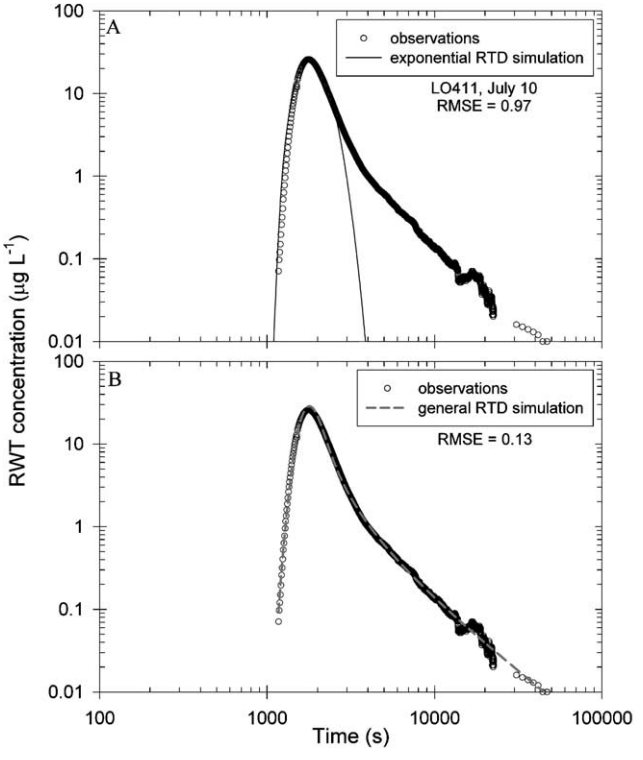

Fig. 4. LO411 stream tracer observations and simulation results from July 10, 2001 RWT stream tracer experiment for: (A) exponential RTD modeling and (B) general RTD modeling.

less tracer mass observed entering the reach (51.93 g) than leaving the reach (52.69 g, Table 3). During late-time sampling ($>10^5$ s, July 19, 2001) with automatic sampling equipment, a rain event was observed at two nearby meteorological stations within 24 h of the experiment (2 mm at UPLMET and 0.75 mm at CEN-MET, see http://www.fsl.orst.edu/lter/).

4.3. Alternative comparisons

The cumulative distribution of the mass of tracer recovered at the bottom of the WS03 study reach, and the predicted recovery, based upon exponential and power-law RTDs shows differences between the two models (Fig. 6). The general RTD model slightly overestimates peak concentrations in the advected slug of tracer, leading to a departure between the observed and predicted cumulative mass at early time. At late-time, the general RTD model fits the observed data well, so that the observed and predicted lines are parallel. In contrast, the exponential RTD model underestimates late-time concentrations, so that the differences between observed and predicted data continue to increase until the end of the experiment.

The timescales of several commonly studied biogeochemical processes of stream water in the hyporheic zone are presented relative to $g(t)$ for WS03 (Fig. 7).

Table 2
Parameter estimates and mean residence times for general RTD modeling for WS03 and Lookout Creek experimental reaches

Parameter	Parameter/metric value			
	WS03	LO411 (July 10, 2001)	LO410 (July 18, 2001)	LO411 (July 18, 2001)
RTD type	Power-law	Power-law	Power-law	Power-law
β_{tot}	15.02	4.39	2.54	86.09
	$[1.18 \pm 0.006]$	$[0.642 \pm 0.010]$	$[0.406 \pm 0.018]$	$[1.93 \pm 0.030]$
D ($m^2\ s^{-1}$)	0.102	0.363	0.573	0.275
	$[-0.99 \pm 0.002]$	$[-0.439 \pm 0.008]$	$[-0.242 \pm 0.011]$	$[-0.560 \pm 0.007]$
k	1.30	1.58	1.53	1.33
	$[0.112 \pm <0.001]$	$[0.198 \pm 0.002]$	$[0.185 \pm 0.030]$	$[0.124 \pm 0.002]$
φ	1.13	1.23	1.29	1.00[a]
	$[0.051 \pm 0.003]$	$[0.091 \pm 0.008]$	$[0.110 \pm 0.016]$	
v ($m\ s^{-1}$)	0.118	0.231	0.266	0.184
	$[-0.929 \pm <0.001]$	$[-0.634 \pm 0.004]$	$[-0.575 \pm 0.031]$	$[-0.736 \pm 0.002]$
Metric				
t_S (s)	4.13×10^5	2.96×10^5	3.11×10^5	4.02×10^6
Model fit				
RMSE	0.09	0.13	0.43	0.34

Values in brackets represent log(parameter value) ±95% confidence interval.
[a] Total loss for LO411 on July 18 was set to 1.00.

Table 3
Mass recovery for exponential and general RTD modeling for WS03 and Lookout Creek experimental reaches

Mass (g)	WS03	LO411 (July 10, 2001)	LO410 (July 18, 2001)	LO411 (July 18, 2001)
Injected	11.0	10.4	75.0	75.0[a]
Observed recovery	8.72	8.16	51.93	52.69
Exponential simulated recovery	7.13	6.88	42.17	44.73
General RTD simulated recovery	9.03	8.30	57.70	46.89

[a] Mass injected at the head of Reach 410.

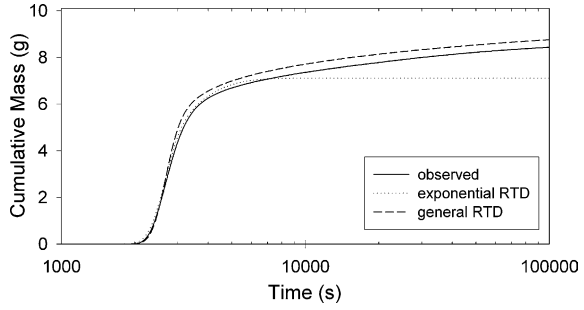

Fig. 6. Cumulative tracer mass passing (CDF * Q) for simulations and observations of WS03.

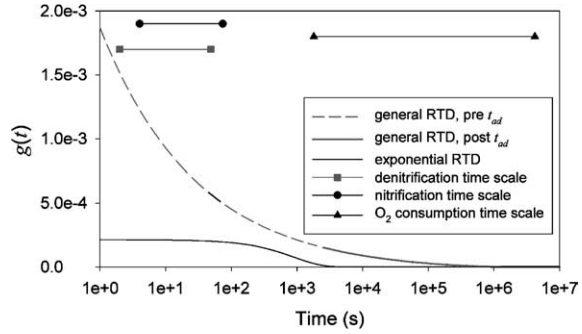

Fig. 7. Approximate timescales of hyporheic biogeochemical reactions and $g(t)$, which is proportional to the probability of a solute molecule being present in the hyporheic zone at time t, for the WS03 experiment.

Recall that the value of $g(t)$ is proportional to the amount of water taking at least that long to exchange with the stream. Reactions operating more slowly than the hyporheic residence time would not have time to go to completion, and so solutes participating in these reactions would not be at equilibrium. Studies of nutrient transformation rates in Pacific Northwestern streams [8,42] and summarized by Triska et al. [43] show that maximum rates of nitrification (115 μg N cm^{-3} sediment h^{-1}) and denitrification (111 μg N cm^{-3} sediment h^{-1}) in nutrient-amended sediment slurries were similar. Typical late summer concentrations of NH_4 and NO_3 in streams of the Lookout Creek watershed are 5 and 8 μg N l^{-1}, respectively [47]. Assuming that the porosity of hyporheic sediment is 0.30, we calculated the time it would take for nitrification or denitrification to consume 5% and 95% of the N available in the pore water of hyporheic sediment. Similarly, soluble reactive phos-

phate (SRP) uptake timescale was calculated from data for streams in the Lookout Creek watershed (7.5 μg Pl^{-1}, H.J. Andrews LTER database, http://www.fsl.orst.edu/lter/), and an uptake rate of 23.15 $pg\,cm^{-2}\,s^{-1}$ [28,31]. Finally, we calculated the timescale for dissolved oxygen (O_2) uptake, as a surrogate for mineralization of organic carbon. We were unable to find comparable uptake rates, so we relied on field observation of the loss of O_2 and median travel times of exchange flows. The resulting O_2 uptake rates ranged widely [11], with as much as 20% of the available O_2 consumed in 360 s [5], to as little as 68% consumed in 33 days [45]. Assuming stream water is 100% saturated, with a concentration of 12 $mg\,l^{-1}$, consumption of O_2 would take as little as 1.8×10^3 s to as long as 4.2×10^6 s in Lookout Creek streams.

5. Discussion

5.1. Comparison between exponential and general RTD models

The results of the WS03 exponential model fit the data well during the advective solute transport peak, but underestimate long residence time storage. The model predicts tracer concentrations should return to background concentrations by $\sim1\times10^4$ s, whereas the observations show that tracer is released from storage at least until $\sim3\times10^5$ s (Fig. 2A). The resulting exponential hyporheic residence time is 882 s (Table 1). This runs counter to the power-law RTD modeling, for which a mean hyporheic residence time cannot be identified, or at least not one that is within the timescale of the tracer experiment [18]. Assuming that the longest timescale of exchange bounds the extent of the power-law RTD, the mean residence time of the general RTD for WS03 is 4.13×10^5 s (Table 2). The power-law RTD fit to the data agrees much better with the observations (Fig. 2B), and suggests that additional tracer mass remains in storage, yet to be released, as observed tracer concentrations have not yet reached background (0 $\mu g\,l^{-1}$) by the end of the tracer experiment (3×10^5 s). Results of the tracer experiments in fourth-order Lookout Creek also show that the general RTD model fit the observed data better than the exponential RTD model (Figs. 3–5). Again, the exponential RTD model fits the observed data quite poorly at late-time, except in the July 18 simulation in LO411. The differences between the model fits do not appear to be as significant in reach LO411 in the July 18 experiment (Fig. 5), but RMSE of the exponential RTD was 0.99, versus 0.34 for the power-law RTD. Because of the rain event during the late time sampling ($>10^5$ s), stream flow increases (which were not recorded) likely diluted observed RWT concentrations. Therefore, both the transient storage and general RTD model fits are suspect at very late-time in the Lookout Creek reaches (LO410 and LO411).

The substantially improved model fits in WS03, LO410, and LO411 on July 10 using a power-law RTD suggest that the exponential RTD assumption is not valid for characterizing the hyporheic exchange response at late time in these three mountain stream reaches, using the slug RWT tracer technique. Further, the three stream reaches studied varied greatly in the types and relative abundances of morphologic features that drive hyporheic exchange flows and create transient storage. That the exponential RTD model provided relatively poor fits to the observed late-time data in all three stream reaches suggests that the assumption of exponentially distributed residence times may not be valid in many types of mountain streams. Comparisons of stream RWT data and solute transport simulations are facilitated at late-time by the log–log plots (Figs. 2–5).

5.2. Interpretation of OTIS and STAMMT-L model parameters

The three stream reaches studied are geomorphically distinct. We expected substantial differences in parameter values for comparison of each RTD simulation, and model parameters from both models showed substantial differences among reaches. However, interpretation of the parameters and their implications for physical differences in the relative importance of the hyporheic zone among the three reaches is difficult.

In OTIS, the influence of advective transport through the stream channel, and the influence of transient storage are described by the cross-sectional areas of the stream channel and the transient storage zone, respectively. Some transient storage results from slack-water environments in the surface stream channel, but in mountain streams, most transient storage is thought to derive from hyporheic exchange. The importance of transient storage relative to stream size is commonly expressed as the ratio, A_S/A, because comparisons between different streams are confounded by differences in stream size. In the STAMMT-L model, the parameter β_{tot} reflects the ratio of the relative sizes of the zone of identifiably slower solute transport to the zone of faster (advective) transport, and thus is roughly analogous to A_S/A.

The OTIS model uses the exchange coefficient, α, to describe exchange of water between the stream and the transient storage zone. In contrast, the STAMMT-L model, with a power-law RTD, uses the parameter k to fit the slope of the late-time data, and thus characterizes late-time exchange flow, beyond the advected pulse of tracer. Larger values of k represent a steeper slope of late-time solute concentrations versus time, and thus are indicative of relatively less long-term storage because of a more rapid return to background concentrations.

Finally, the OTIS model can account for adsorption of a non-conservative solute like RWT, using the first-order uptake coefficient, λ. STAMMT-L does not account for tracer adsorption, but does include a dilution factor, φ that allows loss of tracer mass from the model simulation. The dilution factor should not be confused with lateral groundwater inputs ($q_{\text{lat-in}}$), which can be simulated in OTIS (see [34]) because it accounts for a true loss of mass, as if the tracer is permanently sorbed to streambed sediment, or missing due to bypassing underflow of hyporheic water.

OTIS does have a clear advantage over STAMMT-L in modeling several reaches in series. In this study, each reach was modeled independently, so as to be consistent between the modeling approaches. STAMMT-L currently cannot model changing stream parameters in space.

5.3. Comparison of WS03 and Lookout Creek modeling results

We expected that transient storage would be much greater in reach LO411 than in reach LO410. Previous work on these and other streams in the Lookout Creek watershed [25,46] suggest that morphologically complex stream reaches with secondary channels, or braided channels, support much larger hyporheic zones than would be present in similar sized streams with single thread channels. The results of the tracer experiments in fourth-order Lookout Creek, and analysis with both models supported our expectations. The exponential RTD model showed that both A_S and the A_S/A ratio in reach LO411 were nearly 10-fold larger than in reach LO410 on July 18, and 3-fold larger in the July 10 experiment. Similarly, the STAMMT-L parameter, β_{tot}, suggests that the relative size of the hyporheic zone is much larger in LO411 than in LO410 for both LO411 simulations. The larger value for k found in LO410 compared to LO411 on July 18 is not surprising, as exchange flows are driven primarily by pool-step sequences which create relatively short flow paths, and therefore have shorter timescale RTDs. Conversely, exchange flows between widely spaced, braided channels such as those present in LO411 are long, and therefore create RTDs that are relatively long and should result in a smaller k. The larger k value found in LO411 on July 10 compared to LO410 is surprising though.

The two models do not agree on the size of the transient storage zone in WS03, relative to the other stream reaches studied. Previous studies have found that the relative size of the transient storage zone (A_S/A) is larger in small streams than in big streams, or larger at low discharge than at high discharge [7,25,30]. The exponential RTD simulation suggests that the transient storage zone was smallest in WS03 (Table 1), whereas the general RTD model results suggest that it was intermediate among the three fourth-order reach simulations, but larger than LO410 and LO411 in the July 10 experiment (Table 2). Examination of the model fits show that the exponential RTD greatly underestimates late-time transient storage in WS03 (Fig. 2) and thus fails to account for a significant proportion of the tracer mass moving through the stream reach (Table 3). It seems reasonable to expect that the size of the transient storage zone, relative to stream discharge, is larger in WS03 than in LO410. Reach LO410 is characterized by a single thread channel with widely spaced pool-step (or pool-riffle) channel units. In contrast, pool-step features formed by boulders, logs, and logjams are frequent in WS03, often spaced only a few meters apart. Additionally, there are several small side channels, or secondary channels, present in WS03. Pool-step features are primary drivers of hyporheic exchange flow in mountain streams [20,25] and should drive large volumes of hyporheic exchange flow in WS03.

Both models suggest that the size of the transient storage zone in LO411 on July 18 is much larger than in WS03. Further, the close match in the STAMMT-L model parameter, k, suggests that the relative proportion of long-residence time exchange flows are similar in both reaches. However, the channel morphologies of the two reaches are wildly dissimilar (Fig. 1). An analysis of hyporheic exchange flows in WS03 using a groundwater flow model Kasahara and Wondzell [25], show that pool-step sequences drive high rates of hyporheic exchange flow and that turn-over lengths of stream water were less than 100 m in WS03 at summer low flow. Further, the pool-step sequences tended to drive exchange flows with relatively short RTDs, although some long residence time exchange flows were observed, created by stream water captured in down valley trending flow paths that only return to the stream at the bottom of the study reach where bedrock constraint forces water back to the stream. Kasahara and Wondzell [25] also simulated subsurface flows through a large, unconstrained reach of Lookout Creek, several kilometers downstream of reach LO411. Simulations documented an extensive hyporheic zone with abundant exchange flows. However, stream discharge was proportionally much greater, resulting in a turnover length of 1.69 km. Secondary channels drove exchange flows that extended for 25 to 50+ m, across the full width of the active floodplain, resulting in proportionally longer residence time exchange flows than in WS03.

Given our previous work, and our current understanding of the ways in which channel morphologic features drive hyporheic exchange flows, we are unable to explain why both the exponential and power-law RTD models estimate a large size for the transient storage zone in LO411 in the July 18 experiment, but with a late-time RTD similar to that of WS03. LO411 does have a steeper longitudinal gradient (4%) than

the unconstrained reach of middle Lookout Creek studied with a groundwater flow model (2%) [25]. Also, the spatial scale of features is smaller in LO411, where braided channels are separated by 10–25 m, rather than 25–50 m as in middle Lookout Creek. We have yet to analyze hyporheic exchange flows in a reach like LO411 with a groundwater flow model. Perhaps the steeper gradients and smaller spatial scale do, in fact, create large volumes of transient storage in fourth-order streams, but with RTDs similar to those of steep, second-order streams like WS03. Alternatively, unexpected values of model parameters for LO411 may be strongly influenced by the design of our tracer experiment. The break between reaches LO410 and LO411 is not located on bedrock. We suspect that some tracer mass bypassed the sampling station at the bottom of LO410 in subsurface flows. Because the sample station at the bottom of LO411 was located at a channel spanning bedrock outcrop, we assume that all hyporheic flow paths were forced to return to the stream. Thus more tracer mass was recovered at LO411 than in the upstream reach, LO410 (Table 3). The influence of this "unaccounted tracer mass" on the model fit and resulting parameter values is unknown. The LO411 general RTD modeling for the July 18 experiment suggests a very large β_{tot} value, an order of magnitude higher than others found here (Table 2). The general RTD model parameters found for LO411 on July 18 are likely in error because of the mismatch in upstream and downstream RWT mass recovery (Table 3). On the other hand, the results of the LO411 experiment on July 10 need not be tempered by such complications. Therefore, we consider the comparison of LO410 and the LO411 data from July 10 to be a more reasonable comparison. It is interesting to note the differences in model performance based on the differing experimental conditions.

5.4. Importance of long residence time hyporheic exchange flows in stream ecosystem processes

The results presented here suggest that conventional advection–dispersion and one-dimensional transport models using an exponential RTD may underestimate long residence time hyporheic exchange flows. An important question remains, however, as to the importance of these exchange flows in stream ecosystem processes. Much of the recent interest in the hyporheic zone stems from increased awareness that biogeochemical processes occurring in the hyporheic zone may have large influences on streams. The potential influence of hyporheic exchange flows will be determined by (1) the volume and residence time of stream water flowing through the hyporheic zone, and (2) the time-rate of the biogeochemical process of interest. In general, the role of water with long residence times is not believed to substantially influence stream ecosystems because the volume of water is small, relative to stream discharge. However, if residence times commonly follow power-law distributions the volume of long-residence time water may be much larger than previously thought.

The time-rate of nutrient transformations determine the influence that hyporheic exchange flows of different residence times will have on stream nutrient cycles. Long-residence times are unnecessary to support biogeochemical processes occurring at fast rates. For example, nitrification, and uptake of soluble reactive phosphorous occurs rapidly in most streams (Fig. 7) [43]. Thus, these processes reach completion (or reach equilibrium concentrations) over very short distances so that short-residence time flow paths may be sufficient for these processes to occur. Processes that occur more slowly, however, have the potential to be strongly affected by long-residence time exchange flow paths. For example, mineralization of dissolved organic carbon (DOC) and nitrogen (DON), as indicated by loss of dissolved oxygen (Fig. 7) may occur over timescales of days to weeks [11] and therefore has the potential to be strongly influenced by long-residence time exchange flow paths. Denitrification rates are rapid under optimal conditions, and anaerobic environments are favorable. Thus, denitrification may also be strongly influenced by long-residence time exchange flow paths along which O_2 is consumed. Relative to the probability of tracer presence in the hyporheic zone, transport timescales, which are characterized differently for exponential or power-law RTD, appear to be very important according to Fig. 6.

5.5. Future directions

Similar to the findings of Bencala et al. [1], we found that RWT was not an ideal conservative tracer, as no more than 80% of the injected mass was recovered downstream (Table 3) in any of the three experiments presented here. RWT was chosen as a useful tracer in this study because of the very low detection limit (0.01 $\mu g\,l^{-1}$) and the precise data that could easily be obtained in the field. Conventional salt tracers cannot provide the resolution needed to examine the late-time concentration data, which we argue has much value in defining the entire hyporheic RTD. On the other hand, salt tracers are generally more conservative [50]. The search for an alternative tracer that is non-toxic, conservative, and offers precision and ease of sampling like RWT, is certainly warranted.

The biogeochemical timescales presented here are approximate and may or may not be representative of true nutrient dynamics in these particular systems. Additionally, hyporheic flow paths are not static, as was

assumed here in the biogeochemical timescale computations. The point made here is to illustrate that an improved understanding of solute movement and the quantity of solute moving are of great interest in studies of biogeochemical cycling. Thus, an investigation into biogeochemical cycling in streams using the technique presented here is appropriate.

6. Conclusions

The exponential and general RTD models presented here both have limitations. While the exponential RTD model has become popular in hyporheic exchange studies, we conclude that the exponential RTD model is not appropriate for characterizing late-time behavior of the stream tracer experiments reported here. Unfortunately, the limitations of the exponential RTD model are rarely considered and the use of salt tracers to characterize hyporheic exchange does not provide adequate late-time data because of background solute concentrations and analysis precision.

The general RTD model was shown to be superior in late-time breakthrough curve modeling, but it has limitations at the timescale of advective transport. We propose that there may be reason to combine differing RTD models based on the data presented here. Early portions of the breakthrough curves appear to be better characterized by the exponential RTD model, whereas late-time portions of the breakthrough curve are better characterized by the power-law RTD. This may be an indication that short timescale flow paths, whether they are hyporheic or in-stream transient storage zones, are better characterized by solute transport assumed by the exponential RTD, while longer timescale exchange processes are subject to a power-law distribution of residence times. In addition, owing to the current lack of a fail-safe, user-friendly code and the more challenging mathematics of the general RTD model, the general RTD model is still somewhat cumbersome to employ.

We contend that the late-time portion of the breakthrough curve yields the most information about hyporheic exchange processes. Thus, characterizing longer timescale hyporheic exchange more accurately may be critical to the study of hyporheic biogeochemical processes. We recommend that models should be compared to elution data in log(concentration) space at late-time, where data are most sensitive to hyporheic exchange, so that differences may be easily seen.

The non-conservative transport of RWT continues to be a challenge in stream tracer experiments, as mass loss results in model parameter errors. The search for an alternative tracer that is conservative, non-toxic, and offers ease of use and high precision at low concentration is certainly warranted.

Acknowledgements

The authors would like to gratefully acknowledge Lindsey Treon, Michael Hughes, Matt Johnson, and Teachers in the Woods: Adam Matot, Gary Miller, and Deborah Frankel for assistance with field work; Randy Wildman, John Selker and Jim Wiggington for loan of field equipment. Stream discharge data were provided by the Forest Science Data Bank, a partnership between the Department of Forest Science (Oregon State University) and the Pacific North West Research Station (USDA Forest Service), Corvallis. This work was supported by funding from the National Science Foundation's Hydrologic Sciences Program through grant EAR-9909564. Additional funding was provided by the Pacific North West Research Station and the H.J. Andrews Long-Term Ecological Research program.

References

[1] Bencala KE, Rathbun RE, Jackman AP, Kennedy VC, Zellweger GW, Avanzino RJ. Rhodamine WT dye losses in a mountain stream environment. Water Resour Bull 1983;19(6):943–50.
[2] Bencala KE, McKnight DM, Zellweger GW. Characterization of transport in an acidic and metal-rich mountain stream based on a lithium tracer injection and simulation of transient storage. Water Resour Res 1990;26(5):989–1000.
[3] Bencala KE. Hyporheic zone hydrological processes. Hydrol Proc 2000;14:2797–8.
[4] Bencala KE, Walters RA. Simulation of solute transport in a mountain pool-and-riffle stream: a transient storage model. Water Resour Res 1983;19(3):718–24.
[5] Brestchko G. The limnology of a low order alpine gravel stream (Ritrodat–Lunz stuey area, Austria). Int Ver Theor Agnew Limnol Verh 1991;24:1908–12.
[6] Chapra SC, Runkel RL. Modeling impact of storage zones on stream dissolved oxygen. J Environ Eng 1999;125(5):415–9.
[7] D'Angelo DJ, Webster JR, Gregory SV, Meyer JL. Transient storage in Appalachian and Cascade mountain streams as related to hydraulic characteristics. J N Am Benthol Soc 1993;12(3):223–35.
[8] Duff JH, Triska FJ. Denitrification in sediments from the hyporheic zone adjacent to a small forested stream. Can J Fish Aquat Sci 1990;47:1140–7.
[9] Elliott AH, Brooks NH. Transfer of nonsorbing solutes to a streambed with bed forms: theory. Water Resour Res 1997;33(1):123–36.
[10] Elliott AH, Brooks NH. Transfer of nonsorbing solutes to a streambed with bed forms: laboratory experiments. Water Resour Res 1997;33(1):137–51.
[11] Findlay S. Importance of surface–subsurface exchange in stream ecosystems: the hyporheic zone. Limnol Oceanogr 1995;40(1):159–64.
[12] Gooseff MN, McKnight DM, Lyons WB, Blum AE. Weathering reactions and hyporheic exchange controls on stream water chemistry in a glacial meltwater stream in the McMurdo Dry Valleys. Water Resour Res 2002;38:1279 [doi:1210.1029/2001WR000834].
[13] Grant GE, Swanson FJ. Morphology and processes of valley floors in mountain streams, western Cascades, Oregon. In: Grant Costa JE, Swanson Miller AJ, Potter KW, Wilcock P, editors. Natural and anthropogenic influences in fluvial geomorphology.

Geophysical Monograph Series. Washington, DC: American Geophysical Union; 1995. p. 83–101.
[14] Gregory SV, Swanson FJ, McKee WA. An ecosystem perspective of riparian zones. Bioscience 1991;41:540–51.
[15] Haggerty R, Gorelick SM. Multiple-rate mass transfer for modeling diffusion and surface reactions in media with pore-scale heterogeneity. Water Resour Res 1995;31(10):2383–400.
[16] Haggerty R, McKenna SA, Meigs LC. On the late-time behavior of tracer test breakthrough curves. Water Resour Res 2000;36(12): 3467–80.
[17] Haggerty R, Reeves P. STAMMT-L version 1.0 user's manual. Albuquerque NM: Sandia National Laboratories; 2002. 76 p. [ERMS #520308].
[18] Haggerty R, Wondzell SM, Johnson MA. Power-law residence time distribution in the hyporheic zone of a 2nd-order mountain stream. Geophys Res Let 2002;29(13) [doi:10.1029/2002GL014743].
[19] Hart DR. Parameter estimation and stochastic interpretation of the transient storage model for solute transport in streams. Water Resour Res 1995;31(2):323–8.
[20] Harvey JW, Bencala KE. The effect of streambed topography on surface–subsurface water exchange in mountain catchments. Water Resour Res 1993;29(1):89–98.
[21] Harvey JW, Wagner BJ, Bencala KE. Evaluating the reliability of the stream tracer approach to characterize stream–subsurface water exchange. Water Resour Res 1996;32:2441–51.
[22] Helsel DR, Hirsch RM. Statistical methods in water resources. Amsterdam: Elsevier; 1992. 529 p.
[23] Ho RT, Gelhar LW. Turbulent flow with wavy permeable boundaries. J Fluid Mech 1973;58:403–14.
[24] Jackman AP, Walters RA, Kennedy VC. Transport and concentration controls for chloride, strontium, potassium and lead in Uvas Creek, a small cobble-bed stream in Santa Clara County, California, USA. 2. Mathematical modeling. J Hydrol 1984;75: 111–41.
[25] Kasahara T, Wondzell SM. Geomorphic controls on hyporheic exchange flow in mountain streams. Water Resour Res 2003;39:1005 [doi:1010.1029/2002wr001386].
[26] Laenen A, Risley JC. Precipitation-runoff and streamflow-routing model for the Willamette River Basin. US Geological Survey Water-Resources Investigations Report 95-4284, Oregon; 1997.
[27] Marquardt DW. An algorithm for least-squares estimation of nonlinear parameters. J Soc Ind Appl Math 1963;11(2):431–41.
[28] Meals DW, Levine SN, Wang D, Hoffmann JP, Cassell A, Drake JC, et al. Retention of spike additions of soluble phosphorus in a northern eutrophic stream. J N Am Benthol Soc 1999;18(2):185–98.
[29] Montgomery DR, Buffington JM. Channel-reach morphology in mountain drainage basins. GSA Bull 1997;109(5):596–611.
[30] Morrice JA, Valett HM, Dahm CN, Campana ME. Alluvial characteristics, groundwater–surface water exchange and hydrological retention in headwater streams. Hydrol Proc 1997;11:253–67.
[31] Munn NL, Meyer JL. Habitat-specific solute retention in two small streams: an intersite comparison. Ecology 1990;71:2069–82.
[32] Packman AI, Bencala KE. Modeling surface–subsurface hydrological interactions. In: Jones JB, Mulholland PJ, editors. Streams and ground waters. San Diego, USA: Academic Press; 2000. p. 45–80.
[33] Poeter EP, Hill MC. Documentation of UCODE, a computer code for universal inverse modeling. Water Resources Investigation Report 98-4080. US Geological Survey, Denver, CO; 1998.
[34] Runkel RL. One-dimensional transport with inflow and storage (OTIS): a solute transport model for streams and rivers. US Geological Survey Water Resources Investigations Report 98-4018; 1998.
[35] Runkel RL, McKnight DM, Andrews ED. Analysis of transient storage subject to unsteady flow: diel flow variation in an Antarctic stream. J N Am Benthol Soc 1998;17:143–54.
[36] Savant SA, Reible DD, Thibodeaux LJ. Convective transport within stable river sediments. Water Resour Res 1987;23:1763–8.
[37] Scott DT, Gooseff MN, Bencala KE, Runkel RL. Automated calibration of a stream solute transport model: implications for interpretation of biogeochemical parameters. J N Am Benthol Soc, in press.
[38] Tate CM, Broshears RE, McKnight DM. Phosphate dynamics in an acidic mountain stream: interactions involving algal uptake, sorption by iron oxide, and photoreduction. Limnol Oceanog 1995;40:938–46.
[39] Thackston EL, Schnelle Jr KB. Predicting effects of dead zones on stream mixing. J Saint Eng Div ASCE 1972;96(SA2):319–31.
[40] Thibodeaux LJ, Boyle JD. Bedform-generated convective transport in bottom sediment. Nature 1987;325:341–3.
[41] Triska FJ, Sedell JR, Cromack Jr K. Nitrogen budget for a small coniferous forest stream. Ecol Monogr 1984;54:119–40.
[42] Triska FJ, Duff JH, Avanzio RJ. Influence of exchange flow between the channel and hyporheic zone on nitrate production in a small mountain stream. Can J Fish Aquat Sci 1990;47:2099–111.
[43] Triska FJ, Duff JH, Avanzio RJ. The role of water exchange between a stream channel and its hyporheic zone in nitrogen cycling at the terrestrial–aquatic interface. Hydroboilogy 1993;251:167–84.
[44] Vannote RL, Minshall GW, Cummins KW, Sedell JR, Cushing CE. The river continuum concept. Can J Fish Aquat Sci 1980;37:130–7.
[45] Vervier P, Naiman RJ. Spatial and temporal fluctionations of dissolved organic carbon in subsurface flow of the Stillaguamish River (Washington, USA). Arch Hydrobiol 1993;123:401–12.
[46] Wondzell SM, Swanson FJ. Seasonal and storm dynamics of the hyporheic zone of a 4th-order mountain stream I: hydrological processes. J N Am Benthol Soc 1996;15(1):3–19.
[47] Wondzell SM, Swanson FJ. Seasonal and storm dynamics of the hyporheic zone of a 4th-order mountain stream II: nitrogen cycling. J N Am Benthol Soc 1996;15(1):20–34.
[48] Wörman A, Packman AI, Johansson H, Jonsson K. Effect of flow-induced exchange in hyporheic zones on longitudinal transport of solutes in streams and rivers. Water Resour Res 2002;38(1) [doi:10.1029/2001WR000769].
[49] Wroblicky GJ, Campana ME, Valett HM, Dahm CN. Seasonal variation in surface–subsurface water exchange and lateral hyporheic area of two stream-aquifer systems. Water Resour Res 1998;34(3):317–28.
[50] Zellweger G. Testing and comparison of four ionic tracers to measure stream flow loss by multiple tracer injection. Hydrol Proc 1994;8:155–65.